IOPscience iopscience.iop.org

Home Search Collections Journals About Contact us My IOPscience

Optical absorption and photoluminescence spectra of the ordered defect compound $CuIn_3Te_5$

This article has been downloaded from IOPscience. Please scroll down to see the full text article.

2003 J. Phys.: Condens. Matter 15 3203

(http://iopscience.iop.org/0953-8984/15/19/320)

View the table of contents for this issue, or go to the journal homepage for more

Download details:
IP Address: 171.66.16.119
The article was downloaded on 19/05/2010 at 09:43

Please note that terms and conditions apply.

INSTITUTE OF PHYSICS PUBLISHING JOURNAL OF PHYSICS: CONDENSED MATTER

J. Phys.: Condens. Matter **15** (2003) 3203–3212 PII: S0953-8984(03)59189-5

Optical absorption and photoluminescence spectra of the ordered defect compound $CuIn_3Te_5$

C Rincón[1], S M Wasim[1], G Marín[1], J M Delgado[2] and P M Petroff[3]

[1] Centro de Estudios de Semiconductores, Departamento de Física Facultad de Ciencias, Universidad de Los Andes, Apartado, Postal No 1, La Hechicera Mérida 5101, Venezuela
[2] Centro Nacional de Difracción de Rayos-X, Facultad de Ciencias, Universidad de Los Andes, Apartado, Postal No 40, La Hechicera, Mérida 5101, Venezuela
[3] Materials Department, University of California, Santa Barbara, CA 93106, USA

E-mail: crincon@ula.ve

Received 4 February 2003
Published 6 May 2003
Online at stacks.iop.org/JPhysCM/15/3203

Abstract
The optical properties of the *ordered defect compound* $CuIn_3Te_5$ which crystallizes in a chalcopyrite-related structure have been studied by absorption and photoluminescence (PL) techniques. Optical absorption measurements show that the band gap energy E_G varies from 1.078 to 1.040 eV between 10 and 300 K. It is found that the variation of E_G with temperature is mainly due to the contribution of optical phonons with a characteristic energy of about 16 meV. The PL measurements, carried out between 4 and 100 K with laser excitation intensities in the range from 1 to 400 mW, reveal that the main PL band is due to a donor–acceptor recombination between donor and acceptor defect levels that have activation energies of 60 and 30 meV, respectively. These donor and acceptor states are tentatively assigned as originating from indium atoms on copper sites and copper vacancies, respectively.

1. Introduction

In recent years, information about the physical properties of bulk and thin-film samples of $CuIn_3Se_5$ [1–8] and $CuGa_3Se_5$ [5, 7, 9, 10], which belong to the family of *ordered defect compounds* (ODCs), have started to appear in the literature. The technological interest in these compounds and their mixed alloys [11] has arisen due to the fact that these materials are expected to play an important role in the optimization of the efficiency of $CuInSe_2$–$CuGaSe_2$-based solar cells [12]. From the crystallographic point of view [13], these Cu–III_3–Se_5 ODCs are considered as the fivefold defect derivatives of the II–VI binaries in which the cations are replaced by elements of group I (Cu) and III (In, Ga) and an array of vacancies occupy particular sites in the structure in an orderly manner. Both these ODCs and their alloys crystallize in a chalcopyrite-related structure that has space group

 © 2003 IOP Publishing Ltd Printed in the UK

$P\bar{4}2c$ [11, 14, 15]. On the other hand, Zhang *et al* [4], have suggested that these Cu–III_3–Se_5 ODCs can be derived from the *normal* chalcopyrite Cu–III–Se_2 by introducing a single unit of ordered arrays of (III^{+2}_{Cu} + $2V^{-1}_{Cu}$) donor–acceptor defect pairs (DADPs) in each five units of Cu–III–Se_2.

Study of these ODCs is also of academic importance. This is because they could permit us to understand the role that arrays of vacancies or DADPs play in influencing their crystal structure and electrical and optical properties. Recently, some data on the crystal structure and electrical and optical properties of $CuIn_3Te_5$ [15–18] and $CuGa_3Te_5$ [15, 17], the tellurides corresponding to these ODCs, which also crystallize in the P-chalcopyrite structure [15], have also been published. In the case of $CuIn_3Te_5$, it has been found [18] that at temperatures above around 125 K, the electrical conduction is due to the thermal activation of a shallow acceptor level at around 30 meV due to copper vacancies. In addition, its relatively low hole concentration has been explained as due to the partial annihilation of the shallow acceptor levels originating from copper vacancies in the electrically inactive ($In^{+2}_{Cu} + 2V^{-1}_{Cu}$) DADPs. To explain the temperature dependence of the relatively low charge carrier mobility μ, observed in this compound as compared to its corresponding 1:1:2 phase, a scattering mechanism of the free holes with DADPs has been proposed [18]. The expression for the mobility related to this new scattering mechanism, calculated from simple first principles, when combined with other well-established processes, explains very well the variation of μ with T in the high-temperature activation regime. At low temperatures, the variation of μ with T is explained by means of a variable-range-hopping mechanism of Efros–Shklovskii type.

Hence, continuing our earlier works, in the present article we report on the temperature dependence of the optical absorption and photoluminescence (PL) spectra of $CuIn_3Te_5$.

2. Experimental details

An ingot of $CuIn_3Te_5$ was prepared by the conventional vertical Bridgman technique which is described elsewhere [15]. Circularly shaped void- and crack-free single-crystal samples for optical absorption and PL measurements were cut by slicing it perpendicularly to the growth direction. Although no analysis was made, it is thought that the surface of the samples used in the present study had its orientation very nearly perpendicular to the (112) direction. This is because it is reported [19] that ingots of ternary compound semiconductors having tetragonal chalcopyrite-like structure, grown by the vertical Bridgman technique, have their preferred orientation in this direction. The samples, as checked by a thermal probe, showed p-type conductivity.

Spectra of the optical absorption coefficient α were measured with an automated SPEX 1870 monochromator using a 170 W tungsten lamp as a light source. The transmitted radiation was detected by a cooled PbS detector. For the measurements of α versus $h\nu$ at various temperatures, the sample was placed in a He-cryostat operating in the temperature range from 10 to 300 K.

The PL measurements were performed at several temperatures between 4 and 100 K. For the PL study, the samples, glued on the cold finger of a closed-cycle He cryostat, were excited using a tunable Ti–sapphire laser pumped by an Ar^+-ion laser. The excitation power was varied between 10 and 400 mW. The signal was detected by a liquid-nitrogen-cooled germanium photodetector and analysed with a 0.85 m double-grating spectrometer. Standard lock-in detection was used. Although the PL spectrum does not cover a wide energy range, it was corrected for the response of the detection system to avoid misleading spectral structures.

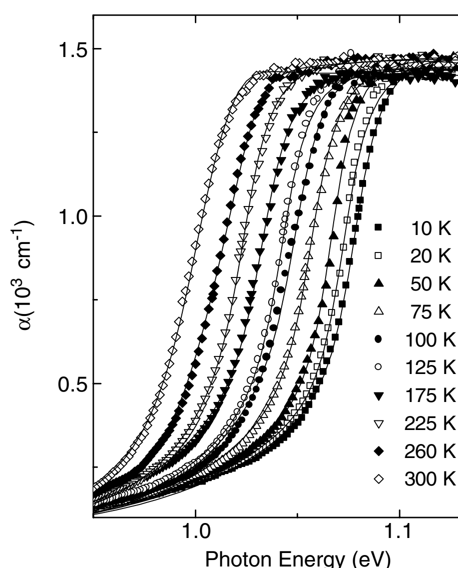

Figure 1. Spectra of the absorption coefficient α of $CuIn_3Te_5$ at various temperatures between 10 and 300 K. The continuous curves represent the fits of equation (1) to the α versus $h\nu$ data.

3. Experimental results and discussion

3.1. Chemical composition and x-ray characterization

The chemical analysis of samples taken from the central part of the ingots, performed by energy-dispersive x-ray (EDX) spectroscopy, gave the representative composition of Cu:In:Te as 10.44:33.60:55.56 at.%, very close to the ideal 1:3:5 value. The error in the standardless analysis was around 5%. However, a slight deficiency of Cu with respect to In ($Cu/In \approx 0.31$) and an excess of Te over cations ($Te/metal \approx 1.26$) is observed. This indicates that the homogeneous 135 phase in the Cu–In–Te system, stable at room temperature, can effectively be formed.

The registered peak positions of the x-ray powder diffraction patterns of $CuIn_3Te_5$ were indexed with a computer program [20]. This analysis produced as the unique solution a tetragonal unit cell corresponding to a chalcopyrite-related structure. The unit-cell parameters $a = 6.1639(3)$ Å and $c = 12.346(2)$ Å were obtained. It is found, as expected, because of the presence of ordered vacancies, that the unit cell parameters of $CuIn_3Te_5$ are smaller by about 0.5% as compared to those of $CuInTe_2$ [21]. It is worth emphasizing that this value lies outside the limit of error in the x-ray measurements in the present case, which is 5×10^{-4} and 2×10^{-3}% for a and c, respectively. Furthermore, this agrees with the trend observed in both Cu–In–Se and Cu–Ga–Se systems, where a and c are smaller by around 0.5% in the 1:3:5 phase than in their corresponding 1:1:2 phases [11].

3.2. Optical absorption measurements

The absorption coefficient spectra, $\alpha(h\nu)$, at different temperatures for a representative $CuIn_3Te_5$ sample, obtained from the transmittance data, are plotted in figure 1. For clarity, α versus $h\nu$ data at 150 and 200 K are not shown. These spectra were analysed with an expression based on Elliot's model for both discrete and continuous excitons [22] which, at a

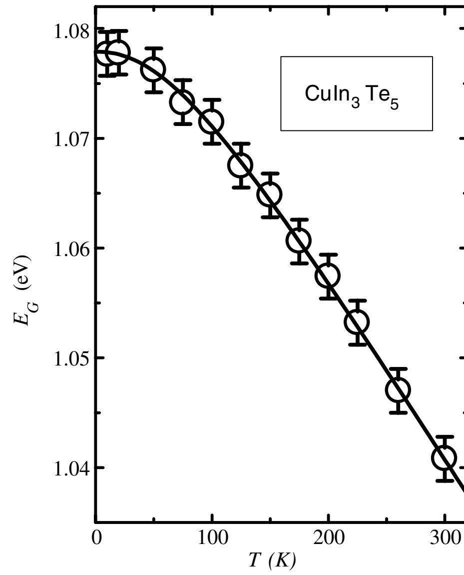

Figure 2. The variation of the energy gap E_G with temperature in $CuIn_3Te_5$. The continuous curve represents the fit of equation (3) to the E_G versus T data with the parameters $E_G(0) \approx 1.078$ eV, $p \approx 2.2$, $\delta \approx 1.7 \times 10^{-4}$ eV K^{-1}, and $\theta \approx 182$ K.

given temperature, is expressed as [6]

$$\alpha(h\nu) = \alpha_0 \sum_n (1/n^3)(\Gamma_n/2)^2/[\Gamma_n/2)^2 + (h\nu - E_G + R_X/n)^2] + \alpha_1\{\pi/2 + \arctan[(h\nu - E_G)/(\Gamma_c/2)]\}, \tag{1}$$

where α_0 represents the absorption peak at the ground state exciton energy and α_1 the absorption at the band gap. Γ_n and Γ_c are the full width at half-maximum of the Lorentzian and the full width of the continuum excitons, and R_X is the free-exciton binding energy. Due to the n^{-3}-dependence of the line intensity of the free-exciton peak, values of the main exciton quantum number n higher than 1 in the summation were neglected.

To obtain the value of the energy gap, equation (1) was fitted to the optical absorption data at each temperature of figure 1 with α_0, α_1, Γ_1, Γ_c, E_G, and R_X as adjustable parameters. For a representative temperature at 10 K, these were 435, 520 cm^{-1}, 41, 23 meV, 1.078 eV, and 7 meV, respectively. It is worth mentioning that, except E_G, all the parameters, as reported earlier for the cases of other semiconductors [18], were found to be very nearly constant with temperature. The variation of the energy gap with T thus obtained is plotted in figure 2.

The temperature variation of E_G in semiconductors is known to be mainly due to the combined contribution of the effect of electron–phonon interaction and that of thermal expansion. The former is the most dominant and contributes about 80–90% to the temperature shift of E_G. Several models [23–25] have been proposed in the literature to describe the temperature variation of the energy gap.

Recently [25], Pässler has presented an analytical description of E_G versus T within the regime of dominance of the electron–phonon interaction. According to his theory, this variation can be given by an integral of the form

$$E_G(T) = E_G(0) - \int f(\varepsilon)\bar{n}(\varepsilon, T)\,\mathrm{d}\varepsilon, \tag{2}$$

where ε is the phonon energy, and $\bar{n}(\varepsilon, T) = [\exp(\varepsilon/k_BT) - 1]^{-1}$ represents the average phonon occupation number. The electron–phonon spectral function $f(\varepsilon)$, in the energy range from 0 to a cut-off value $\varepsilon_{co} = [(\eta+1)/\eta]k_B\theta$, is given by a power law dependence of the form $f(\varepsilon) \propto \varepsilon^{\eta}$. The characteristic temperature θ corresponds to the mean frequency of the phonon spectrum. This is expected to be slightly smaller than the Debye temperature θ_D ($\theta \approx \frac{3}{4}\theta_D$). For exponents within a range from $1.2 < \eta < 1.8$, which corresponds to moderately concave spectral functions, equation (2) takes the form [25]

$$E_G(T) = E_G(0) - (\delta\theta/2)([1 + (2T/\theta)^p]^{1/p} - 1), \tag{3}$$

where δ corresponds to the high-temperature limit, $S(\infty)$, of the associated entropy, and the parameter $p = \eta + 1$. The exponent η governs the shape of the spectral function.

Equation (3) was fitted to the $E_G(T)$ data of figure 2. Values of different parameters obtained by the fit are $E_G(0) = 1.078 \pm 0.001$ eV, $p = 2.2 \pm 0.1$, $\delta = (1.7 \pm 0.3) \times 10^{-4}$ eV K^{-1}, and $\theta = 182 \pm 32$ K. The theoretical curve from this equation is shown in the same figure as a continuous line. A cut-off phonon energy $\varepsilon_{co} \approx 29$ meV ($\sim$234 cm^{-1}) and an effective phonon energy $\varepsilon_{ef} = k_B\theta \approx 16$ meV ($\sim$130 cm^{-1}) are also obtained from the parameters of the Pässler model. It is observed that this cut-off energy is in excellent agreement with the highest-frequency mode at 236 cm^{-1} obtained from Raman spectra [16]. On the other hand, in the absence of the reported frequency of the acoustic phonon modes, the mean frequency of the vibrational modes in $CuIn_3Te_5$ is estimated by considering only the Raman-active modes reported in [16]. The relation used is $\bar{\nu} \approx \sum I_i\nu_i / \sum I_i$, where ν_i and I_i are the frequency and relative intensity of the ith Raman mode, respectively. This gives $\bar{\nu} \approx 128$ cm^{-1} ($\varepsilon \approx 16$ meV), which agrees completely with the effective phonon energy $k_B\theta \approx 16$ meV obtained from the Pässler model. This coincidence indicates that the major contribution of phonons to the shift of E_G versus T in $CuIn_3Te_5$ arises mainly from optical phonons. In addition, from the expression $\theta \approx \frac{3}{4}\theta_D$, the Debye temperature is estimated to be 243 ± 40 K. This value is in agreement with $\theta_D = 179 \pm 20$ K calculated [26] from the bulk modulus by using a modified version of the square-root law of Madelung and Einstein.

3.3. Photoluminescence measurements

The PL spectra in the energy range from 0.95 to 1.06 eV were obtained between 4 and 100 K at different excitation intensities from 1 to 400 mW. A PL band, centred at $E_P \approx 1.00$ eV, at 4 K and at excitation intensity P_I of 1 mW, is observed in figure 3. As can be seen in the same figure, the energy E_P at which the maximum in the band occurs shifts to higher values with increasing excitation intensity. This can also be appreciated in the plot of P_I versus E_P at 4 K in figure 4. It is also observed in this figure that the shift of E_P to higher energies with P_I tends to saturate around 1.018 eV at values of P_I higher than about 200 mW. This is typical of the donor–acceptor pair (DAP) recombination. It is well known that the DAP recombination occurs at [27]

$$h\nu \approx E_G - (E_D + E_A) + e^2/\varepsilon_0 r, \tag{4}$$

where E_D and E_A are the activation energies of donor and acceptor levels, respectively, involved in the recombination, r is the separation between the pairs, and ε_0 is the static dielectric constant.

An expression that relates E_P for the DAP recombination to the excitation power P_I, for the case of weakly compensated semiconductors, is given by [28]

$$P_I(E_P) = P_{I0}[(E_P - E_\infty)^3 \exp(-2E_B/(\hbar\omega - E_\infty)]/(E_B + 2\hbar\omega - E_\infty), \tag{5}$$

where P_{I0} is a proportionality constant, E_B is the photon energy emitted by a nearby DAP separated by a shallow impurity Bohr radius $R_B = r$, and E_∞ is the photon energy emitted by

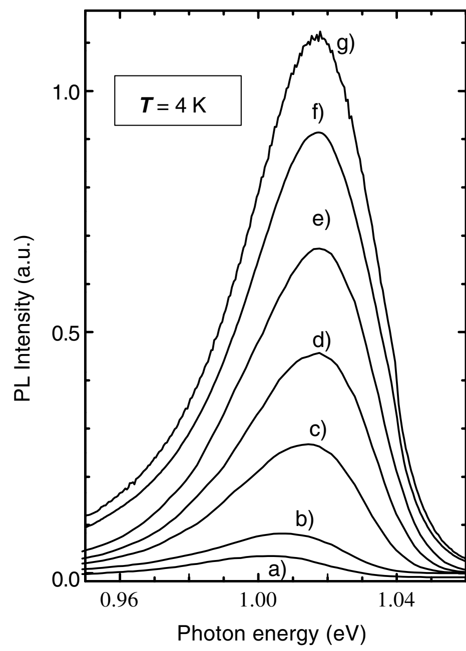

Figure 3. PL spectra of $CuIn_3Te_5$ at 4 K, at various excitation intensities: (a) 1 mW, (b) 5 mW, (c) 20 mW, (d) 50 mW, (e) 100 mW, (f) 200 mW, (g) 300 mW, and (h) 400 mW. The energies of the peak E_P at these excitation intensities are: (a) 1.004 eV, (b) 1.009 eV, (c) 1.014 eV, (d) 1.015 eV, (e) 1.016 eV, (f) 1.017 eV, (g) 1.018 eV, and (h) 1.018 eV.

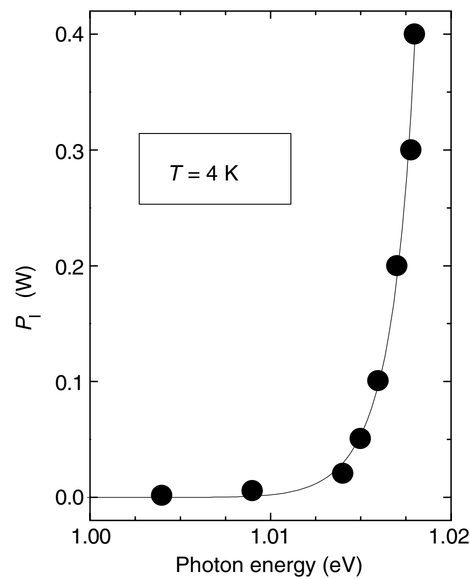

Figure 4. Excitation intensity P_I as a function of the energy of the main peak E_P at 4 K. The best fit of equation (5) to the P_I versus E_P data with $E_\infty \approx 0.988$ eV and $E_B \approx 1.048$ eV is shown by the continuous curve.

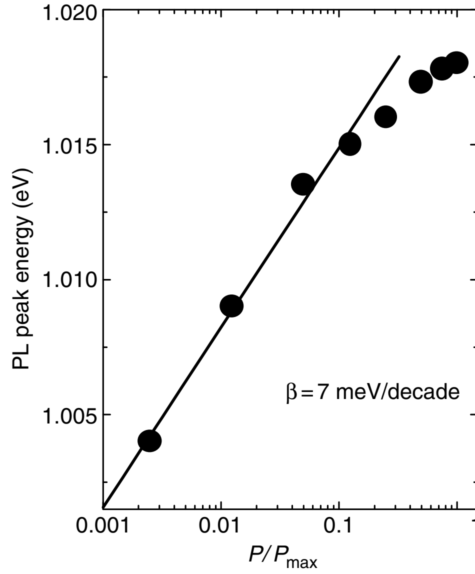

Figure 5. Energy of the main peak E_P as a function of log $P_I/P_{I\,max}$ at 4 K. A blue-shift of the peak energy with increasing P_I, in the low-excitation-intensity range, $\beta \approx 7$ meV/decade, is obtained for this peak.

an infinitely distant DAP. From the fit of equation (5) to the P_I versus E_P data shown in figure 4 by the continuous line, we find $E_\infty = 0.988 \pm 0.009$ eV and $E_B = 1.048 \pm 0.004$ eV. From these values and equation (4), $e^2/\varepsilon_0 R_B$ is estimated to be 60 meV. Then, using $\varepsilon_0 \approx 12$ for $CuIn_3Te_5$ [18], we find $R_B \approx 20$ Å. On the other hand, using the relation $E_\infty \approx E_G - (E_D + E_A)$ with $E_G = 1.078 \pm 0.001$ eV, obtained from the analysis of the absorption data at 10 K, we get $(E_D + E_A) = 0.09 \pm 0.01$ eV.

The shift of E_P to higher energy with increasing P_I is related to the fact that distant pairs saturate more readily with excitation power than the nearby pairs. When E_P is plotted in figure 5 as a function of log $P_I/P_{I\,max}$ ($P_{I\,max} = 400$ mW), a blue-shift β of the peak energy with increasing P_I of about 7 meV/decade is observed for values of P_I lower than 200 mW. For the DAP recombination, shifts of 2–3 meV/decade are usually found for extremely pure and non-compensated materials, and in the range 7–10 meV/decade for more compensated samples [29]. Since in the present case 7 meV/decade lies in this range, it is confirmed that this emission is due to the DAP recombination. It is worth mentioning that the so-called quasi-DAP transitions [30], generally observed in highly doped and compensated semiconductors [29, 31], can be neglected. This is because quasi-DAP emission bands are strongly dependent on the excitation intensity, and values of β of about 20 meV/decade are usually expected [29–31].

It is also observed in figure 6 that the integrated PL intensity I of this band also increases with increasing P_I. The analysis of the data has been carried out by fitting the variation of the integrated PL intensity I with P_I to the simple relation

$$I \propto P_I^\gamma, \tag{6}$$

where γ is a dimensionless constant. It was found that the maximum PL intensity of the emission band increases sublinearly with P_I. The best fit, shown by the solid line, was obtained with $\gamma \approx 0.61$. It is a well-known fact that for the laser excitation with energy exceeding the band gap energy, the coefficient γ is in the range $1 < \gamma < 2$ for the free- and bound-exciton

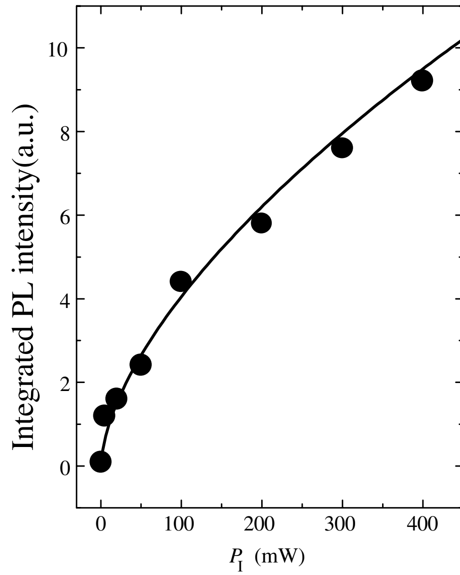

Figure 6. Integrated PL intensity I as a function of the excitation intensity P_I at 4 K. The best fit of equation (6) to the I versus P_I data with $\gamma \approx 0.61$ is shown by the continuous curve.

emissions, and $\gamma < 1$ for free-to-bound and DAP recombinations. The fact that γ is less than one further confirms that the PL emission is due to the DAP recombination [32].

The integrated PL intensity I is plotted in figure 7 as a function of $100/T$. It can be observed that above about 30 K, the emission band intensity decreases very quickly with increasing temperature. This rapid thermal quenching of the PL band can be described by the expression [27]

$$I(T) = I(0)[1 + C\exp(-E_T/k_BT)]^{-1} \tag{7}$$

where C is a constant and E_T the thermal activation energy. The value of $E_T = 30 \pm 3$ meV was obtained by fitting equation (7) to the $I(T)/I(0)$ data.

3.4. Identification of the observed defect levels

The value of $E_T = 30 \pm 3$ meV agrees quite well with the acceptor level at $E_A = 30 \pm 4$ meV obtained from electrical measurements [18]. Both of these values are also in good agreement with the activation energy of the acceptor level $E_A \approx 35$ meV, calculated from the expression [33, 34] $E_A(N) = E_{A0} - \beta N^{1/3}$, that takes into account the effect of screening of the charge carriers by impurities in the activation energy of the shallow acceptor levels. In the calculation, the activation energy $E_{A0} \approx 70$ meV in the dilute limit is estimated by using the hydrogenic model for a single acceptor level ($E_{A0} \approx 13.6m_h^*/m_e\varepsilon_0^2$) with $m_h^* \approx 0.73\, m_e$ and $\varepsilon_0 \approx 12$ [18]. For the screening constant we use $\beta = 3 \times 10^{-8}$ eV cm^{-1}, which is the value obtained for ternary chalcopyrite compounds [35]. The sample in the present work and those used for electrical measurements reported in [18] were obtained from the same disc cut from the ingot. For this reason, the impurity concentration N used in the calculation is taken as the total ionized defect concentration, $N_I = N_A + N_D \approx 1.1 \times 10^{18}$ cm^{-3}, given in [18]. From the EDX analysis it is found that the samples had Cu deficiency and an excess of Te. This deviation from the ideal stoichiometry could lead to the existence of copper vacancies (V_{Cu})

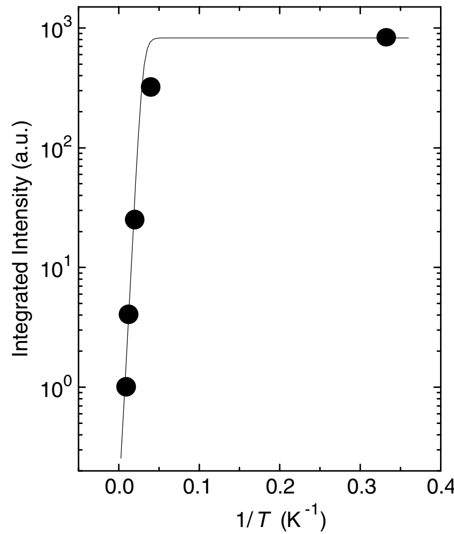

Figure 7. Integrated PL intensity I versus $100/T$ for $CuIn_3Te_5$ at $P = 20$ mW. The best fit of equation (7) to the data with the parameter $E_T \approx 0.03$ eV is shown by the continuous curve.

and tellurium interstitials (Te_i). The former are expected to give rise to single-acceptor states in such semiconducting compounds [36]. Since the estimated activation energy $E_A \approx 35$ meV of a singly ionized acceptor level agrees very well with $E_T \approx 30$ meV obtained from thermal quenching of the PL band and $E_A \approx 30$ meV obtained from electrical data [8] for samples of the same ingot, it is reasonable to conclude that they have the same origin—that is, they are due to the V_{Cu}. On the other hand, the Te_i are expected to give rise to two acceptor levels. The calculated activation energies in the dilute limit for these levels [37] are 1.7 and 4 times higher than that of the single level $E_{A0} \approx 70$ meV. This gives, for the two levels of Te_i, $E_A \approx 120$ and 280 meV; these values are considerably higher than that obtained from the thermal quenching of the PL band and electrical data. This additional evidence allows us to discard the possibility that the level at around 30 meV is due to Te_i. Under this interpretation, assuming that $E_A \approx 30$ meV and that $E_D + E_A \approx 90$ meV, E_D is then calculated to be about 60 meV. Consistent with EDX measurements, this donor level can be attributed to indium interstitials (In_i) or indium on copper sites (In_{Cu}). The value $E_D \approx 60$ meV agrees completely with the activation energy of the second level of the double-donor state In_{Cu}. This is estimated from the expression [36] $E_D \approx 4 \times 13.6(m_e^*/m_0)/\varepsilon_0^2$, where the effective mass of the electron m_e^* in $CuIn_3Te_5$ is taken as $0.16\ m_0$, as for its corresponding 1:1:2 phase [38]. This suggests that the present observed donor level is due to indium on copper site defects.

4. Conclusions

In conclusion, the study of the optical properties of the ODC $CuIn_3Te_5$, which crystallizes in a chalcopyrite-related structure, reveals that the band gap energy decreases with increasing temperature from 1.078 to 1.040 eV in the range between 10 and 300 K. This shift is mainly due to the contribution of optical phonons with an effective phonon energy of about 16 meV. The analysis of the PL data indicates that the main recombination process observed in this material is due to a DAP transition. From the shift of this band to higher energies with excitation power and thermal quenching, an acceptor level located at about 30 meV above the top of the valence

band and a donor level at 60 meV below the bottom of the conduction band, attributed as due to copper vacancies and indium atoms on copper sites, respectively, are identified.

Acknowledgments

This work was supported by grants from FONACIT (Contract Nos G-97000670 and LAB97000821) and CDCHT-ULA (Contract Nos C-917-98-05 and C-918-98-05).

References

[1] Tuttle J R, Albin D S and Noufi R 1991 *Sol. Cells* **30** 21
[2] Schmid D, Ruckh M, Grunwald F and Schock H W 1993 *J. Appl. Phys.* **73** 2902
[3] Nelson A J, Horner G S, Sinha K and Bode M H 1994 *Appl. Phys. Lett.* **64** 3600
[4] Zhang S B, Wei S H, Zunger A and Yoshida H K 1998 *Phys. Rev.* B **57** 9642
[5] Negami T, Kohara N, Nishitani M, Wada T and Hirao T 1995 *Appl. Phys. Lett.* **67** 825
[6] Marín G, Wasim S M, Rincón C, Sánchez Pérez G, Power Ch and Mora A E 1998 *J. Appl. Phys.* **83** 3364
[7] Rincón C, Wasim S M, Marín G, Delgado J M, Huntzinger J R, Zwick A and Galibert J 1998 *Appl. Phys. Lett.* **73** 441
[8] Wasim S M, Marín G, Rincón C and Sánchez Pérez G 1998 *J. Appl. Phys.* **84** 5823
[9] Wei S H, Zhang S B and Zunger A 1998 *Appl. Phys. Lett.* **72** 3199
[10] Rincón C, Wasim S M, Marín G, Hernández E, Sánchez Pérez G and Galibert J 2000 *J. Appl. Phys.* **87** 2293
[11] Marín G, Tauleigne S, Wasim S M, Guevara R, Delgado J M, Rincón C, Mora A E and Sánchez Pérez G 1998 *Mater. Res. Bull.* **33** 1057
[12] Yang L C, Ziao H Z and Rockett A 1994 *J. Appl. Phys.* **76** 1503
[13] Delgado J M 1998 *Ternary and Multinary Compounds (Inst. Phys. Conf. Ser. 152)* (Bristol: Institute of Physics Publishing) p 45
[14] Hönle W, Kühn G and Boehnke U C 1988 *Cryst. Res. Technol.* **23** 1347
[15] Marín G, Delgado J M, Wasim S M, Rincón C, Sánchez Pérez G, Mora A E, Bocaranda P and Henao J A 2000 *J. Appl. Phys.* **87** 7814
[16] Rincón C, Wasim S M, Marín G, Hernández E, Delgado J M and Galibert J 2000 *J. Appl. Phys.* **88** 3439
[17] Rincón C, Wasim S M and Marín G 2002 *Appl. Phys. Lett.* **80** 998
[18] Rincón C, Wasim S M and Marín G 2002 *J. Phys.: Condens. Matter* **14** 997
[19] Rincón C, Wasim S M, Marín G, Hernández E and Galibert J 2001 *J. Phys. Chem. Solids* **62** 20847
[20] Boultif A and Louer D 1991 *J. Appl. Crystallogr.* **24** 987
[21] Wasim S M, Rincón C, Marín G and Delgado J M 2000 *Appl. Phys. Lett.* **77** 94
[22] Elliot R J 1957 *Phys. Rev.* **108** 1384
[23] Varshni Y P 1967 *Physica* **34** 149
[24] Allen P B and Cardona M 1981 *Phys. Rev.* B **23** 1979
[25] Pässler R 1997 *Phys. Status Solidi* b **200** 155
[26] Cáceres J B and Rincón C 2002 *Phys. Status Solidi* b **234** 541
[27] See, for example,
Bebb H and Williams E W 1972 *Semiconductors and Semimetals* vol 8, ed R K Willardson and C E Beer (New York: Academic) p 181ff
[28] Zacks E and Halperin A 1967 *Phys. Rev.* **159** 649
[29] Pavesi L and Guzzi M 1994 *J. Appl. Phys.* **75** 4779
[30] Shklovskii B J and Efros A L 1984 *Electronic Properties of Doped Semiconductors* (Berlin: Springer)
[31] Baucknecht A, Siebentritt S, Albert J and Lux-Steiner M Ch 2001 *J. Appl. Phys.* **89** 4391
[32] Schmidt T, Lischka K and Zulehner W 1992 *Phys. Rev.* B **45** 8989
[33] Pearson G L and Bardeen J 1949 *Phys. Rev.* **75** 865
[34] Lee T F and McGill T C 1975 *J. Appl. Phys.* **46** 373
[35] Neumann H, Nowak E and Kühn G 1981 *Cryst. Res. Technol.* **16** 1369
[36] Polity A, Krause-Rehberg R, Staab T E M, Puska M J, Klais J, Möller J and Meyer B K 1998 *J. Appl. Phys.* **83** 71
[37] Rincón C and Márquez R 1999 *J. Phys. Chem. Solids* **60** 1865
[38] Wasim S M and Albornoz J G 1988 *Phys. Status Solidi* a **110** 575